Periodica Polytechnica
Chemical Engineering

62(2), pp. 215-223, 2018
https://doi.org/10.3311/PPch.10328

Unsteady Convective Diffusion with Interphase Mass Transfer in Casson Liquid

Ashis Kumar Roy[1*], Apu Kumar Saha[1], Sudip Debnath[1]

RESEARCH ARTICLE

Received 26 November 2016; accepted after revision 21 March 2017

Abstract

This study aims to examine the dispersion of a passive contaminant of solute released in Casson liquid flow through a tube. The wall of the tube is taken to be chemically active where the flow is driven by the constant pressure gradient. To evaluate the transport coefficients, Aris-Barton's Moment technique is considered, a finite difference implicit scheme is adopted to handle the differential equation arises in moment methodology. Also to confirm the results obtained by Aris-Barton's method, the generalized dispersion model has been applied. Unlike the previous studies on dispersion in Casson liquid, the time-dependent behavior of the transport coefficients has been established. Some significant observations have been founded, e.g. exchange coefficient is independent of yield stress while the convection coefficient and dispersion coefficient are inversely proportional to yield stress. Results reveal that transport coefficients are enormously affected by wall absorption.

Keywords

casson liquid, longitudinal dispersion, irreversible boundary absorption

[1] Department of Mathematics,
National Institute of Technology Agartala
Tripura, India-799046, India

[*] Corresponding author, e-mail: rk.ashis10@gmail.com

1 Introduction

The process of dispersion is a classical mechanism to measure the rate of spreading of the species in a flowing stream. The studies on dispersion have been extensively applied to chemical engineering [1, 2], environmental protection [3–7] and so many and so forth. The classical attempt of this type of investigation was initiated by Taylor [8] in 1953. He observed that fluid was dispersed about a point moving with mean velocity U of flow with an apparent diffusion coefficient $\frac{a^2U^2}{48D}$ where, D is the molecular diffusion coefficient and a is the radius of the tube, but this is valid only in specific ambiance ($\frac{4L}{A} \gg \frac{Ua}{D} \gg 6.9$, where, L and A be the length and cross-sectional area of the tube respectively). In 1956, Aris [9] generalized Taylor's idea of removing the restrictions imposed by Taylor to include longitudinal diffusion and introduced a new technique called, the "Method of Moment" for measuring the diffusion coefficient on the same geometry. Further, Barton in 1982 [10] identified some technical obstacles in the solution method provided by Aris and resolved them accordingly. Gill and Sankarasubramanian (1971) [11] introduced a different approach known as "Generalized Dispersion Model" to find the effective dispersion coefficient. The authors studied the same where he considered solute reacting with the wall of the pipe. Both Aris-Barton approach and Sankarasubramanian and Gill approach are valid for small as well as large time. Chatwin [12] studied the diffusion of the solute in oscillatory flow. Purtell [13] studied the impact of flow oscillations on the axial diffusion by a perturbation method. Ng [14], and Mazumder and Paul [15] examined dispersion process in presence of reversible and irreversible reactions in the boundary. Imposing the method of integral moments, the analysis of longitudinal dispersion of solute in a periodic flow between two coaxial cylinders was presented by Paul [16] to determine the longitudinal dispersion coefficient with the variation of each of radius ratio, absorption parameter, and frequency parameter. Using asymptotic analysis with respect to pipe thickness, the transport of a reactive solute by diffusion and convection in a thin (or long) curved and circular pipes was considered by Pažanin [17, 18].

The study of dispersion through non-Newtonian fluids has abundant applications in polymer processing, biochemical

processing, and cardiovascular system. In particular, the study of dispersion in Casson fluids has applications in physiological fluid dynamics, chemical engineering etc. Charm and Kurland [19] claimed that under certain specific environment blood behaves like Casson fluid. In 1964, Fan [20] extended the study of Taylor's analysis of Newtonian fluid into a non-Newtonian fluid (Ostwald-de Waele fluid) in a circular tube. He also analyzed the dispersion of solute accompanying the flow of the Bingham Plastic and Ellis model fluid [20] as well and studied the corresponding effect of Taylor's limiting condition on these two models. Sukla [21] investigated the first-order chemical reaction of solute in non-Newtonian fluids flowing through parallel plates and circular tubes by considering the following models: (i) Power law model, (ii) Bingham model, (iii) Casson model. Sharp [22] analyzed the dispersion in non-Newtonian fluids (Casson, Bingham plastic and power law fluids) through conduits using Taylor-Aris dispersion theory which is valid after a large time. This study was extended by Dash et al. [23] for Casson fluids using the generalized dispersion model and they discussed the application of their study in blood flow analysis. Nagarani et al. [24] studied the effect of wall absorption on dispersion in Casson fluid flow in a conduit and extended the theory in an annular pipe in the subsequent paper [25]. In recent days, a large number of articles [26–29] are widely available in the literature to understanding the dispersion process in this respect.

Though a number of attempts on the dispersion of Casson liquid are available in the literature, but all the attempts restricted themselves to study the behavior of transport coefficient under steady state. In the present analysis, we tried to overcome this difficulty and study the time-dependent behavior of transport coefficient.

2 Mathematical Model

A unidirectional, axial, fully-developed flow of an incompressible liquid through a circular pipe of radius $\bar{a}$ is considered.

Fig. 1 shows the flow geometry with cylindrical coordinate system where the axial and radial coordinates are represented by $\bar{z}$ and $\bar{r}$ (bar denotes dimensional quantity). Axi-symmetry is assumed and hence all quantities are independent of θ.

We assume that Casson liquid occupies the region

$$\bar{\Re}_c = \left\{(\bar{r},\bar{z}) : 0 \le \bar{r} \le \bar{a}, -\infty \le \bar{z} \le \infty\right\}. \tag{1}$$

Within the Casson liquid region, plug flow is assumed in the region:

$$\bar{\Re}_p = \left\{(\bar{r},\bar{z}) : 0 \le \bar{r} \le \bar{r}_p - \infty \le \bar{z} \le \infty\right\} \tag{2}$$

The governing equation of motion for the flow in the axial direction is given by

$$-\frac{d\bar{p}}{d\bar{z}} = \frac{1}{\bar{r}}\frac{\partial\left(\bar{r}\bar{\tau}_{\bar{z}\bar{r}}\right)}{\partial\bar{r}}. \tag{3}$$

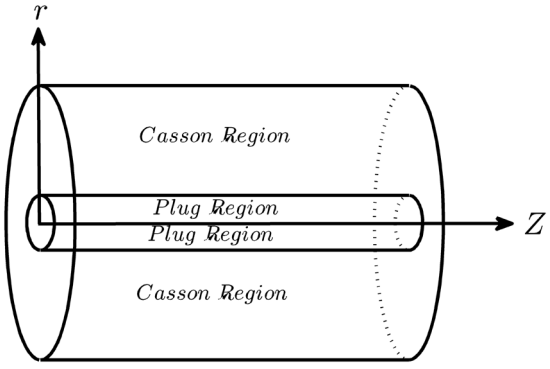

Fig. 1 Flow Geometry

Constitutive equation

$$\left.\begin{aligned} \bar{\tau}_{\bar{z}\bar{r}}^{\frac{1}{2}} &= \bar{\tau}^{\frac{1}{2}} + \left(-\mu_\infty \frac{\partial\bar{u}}{\partial\bar{r}}\right)^{\frac{1}{2}}, && \bar{\tau}_{\bar{z}\bar{r}} \ge \bar{\tau} \\ \frac{\partial\bar{u}}{\partial\bar{r}} &= 0, && \bar{\tau}_{\bar{z}\bar{r}} \le \bar{\tau} \end{aligned}\right\}, \tag{4}$$

where, $\bar{\tau}$ is the yield stress and $\bar{\mu}_\infty$ the Newtonian viscosity of the liquid. From the relation (4), it is obvious that whenever $\bar{\tau}_{\bar{z}\bar{r}} \le \bar{\tau}$, plug flow can be seen.

The boundary conditions are

$$\left.\begin{aligned} &\bar{\tau}_{\bar{z}\bar{r}} \text{ is finite at } \bar{r} = 0, \\ &\bar{u} = 0 \quad \text{at } \bar{r} = \bar{a}, \end{aligned}\right\}. \tag{5}$$

In the uni-directional flow described above, a reactive solute with initial concentration $\bar{C}(0,\bar{r},\bar{z})$ is introduced. The convection-diffusion equation satisfied by the solute concentration $\bar{C}(\bar{t},\bar{r},\bar{z})$ is

$$\frac{\partial\bar{C}}{\partial\bar{t}} + \bar{u}(\bar{r})\frac{\partial\bar{C}}{\partial\bar{z}} = D\frac{\partial^2\bar{C}}{\partial\bar{z}^2} + \frac{D}{\bar{r}}\frac{\partial}{\partial\bar{r}}\left(\bar{r}\frac{\partial\bar{C}}{\partial\bar{r}}\right), \tag{6}$$

where,

$$D = \begin{cases} \bar{D}_1 & \text{for } 0 \le \bar{r} \le \bar{r}_p \\ \bar{D}_2 & \text{for } \bar{r}_p < \bar{r} \le \bar{a} \end{cases}. \tag{7}$$

Here $\bar{r}_p$ is the radius of the plug flow region. $\bar{D}_1$ and $\bar{D}_2$ are the constant molecular diffusivities in the plug flow and Casson liquid region respectively.

The initial and boundary conditions for solving Eq. (6) are:

$$\bar{C}(0,\bar{r},\bar{z}) = C_0 B(\bar{r})\delta(\bar{z}),\ 0 < \bar{r} < \bar{a}, \tag{8}$$

$$\frac{\partial\bar{C}}{\partial\bar{r}} = 0 \text{ at } \bar{r} = 0 \text{ (Symmetry)}, \tag{9}$$

$$\frac{\partial\bar{C}}{\partial\bar{r}} + \bar{\beta}\bar{C} = 0 \text{ at } \bar{r} = \bar{a}, \tag{10}$$

where $\bar{B}(\bar{r})$ is a function of $\bar{r}$ and $\delta(\bar{z})$ is the Dirac delta function. The absorbing boundary condition at the wall of the tube is represented by Eq. (10).

The following dimensionless quantities are used

$$\left.\begin{aligned} t=\frac{\bar{D}_2\bar{t}}{\bar{a}^2}, r=\frac{\bar{r}}{\bar{a}}, z=\frac{\bar{D}_2\bar{z}}{\bar{a}^2u_0}, C=\frac{\bar{C}}{C_0},\\ u=\frac{\bar{u}}{u_0}, u_0=-\frac{\bar{a}^2}{4\mu_\infty}\frac{d\bar{p}}{d\bar{z}},\\ \tau_{zr}=\frac{\bar{\tau}_{\bar{z}\bar{r}}}{\mu_\infty\left(\frac{u_0}{\bar{a}}\right)}, \tau=\frac{\bar{\tau}}{\mu_\infty\left(\frac{u_0}{\bar{a}}\right)}, \end{aligned}\right\}. \tag{11}$$

Using the scaling as in Eq. (11), the initial-boundary value problem (IBVP) given in Eqs. (3) - (10) reduces to:

$$\frac{1}{r}\frac{\partial\left(r\tau_{zr}\right)}{\partial r}=4. \tag{12}$$

$$\left.\begin{aligned} \tau_{zr}^{\frac{1}{2}}=\tau^{\frac{1}{2}}+\left(-\frac{\partial u}{\partial r}\right)^{\frac{1}{2}}\tau_{zr}\geq\tau,\\ \frac{\partial u}{\partial r}=0 \qquad\qquad \tau_{zr}\leq\tau, \end{aligned}\right\}. \tag{13}$$

$$\left.\begin{aligned} \tau_{yz}\text{ is finite at } r=0\\ u=0 \qquad \text{at } r=1 \end{aligned}\right\}. \tag{14}$$

$$\frac{\partial C}{\partial t}+u\left(r\right)\frac{\partial C}{\partial z}=\frac{D^*}{r}\frac{\partial}{\partial r}\left(r\frac{\partial C}{\partial r}\right)+\frac{D^*}{Pe^2}\frac{\partial^2 C}{\partial z^2}, \tag{15}$$

$$D^*=\begin{cases}\dfrac{\bar{D}_1}{\bar{D}_2} & 0\leq r\leq r_p,\\ 1 & r_p\leq r\leq 1.\end{cases} \tag{16}$$

$$\left.\begin{aligned} C\left(0,r,z\right)=B\left(r\right)\psi\left(z\right),\ \left(0<r<1\right)\\ \psi\left(z\right)=\frac{\delta\left(z\right)}{Pe}\\ B\left(r\right)=1 \end{aligned}\right\}. \tag{17}$$

$$\frac{\partial C}{\partial r}=0 \text{ at } \ r=0. \tag{18}$$

$$\frac{\partial C}{\partial r}=-\beta C \text{ at } \ r=1. \tag{19}$$

Here $\beta=\bar{\beta}\bar{a}$ is the absorption parameter or the first order reaction rate and $Pe\left(=u_0\frac{\bar{a}}{\bar{D}_2}\right)$ is the Peclet number that measures the ratio of the characteristic time of the diffusion process to that of the convection process.

3 Solution for the velocity profile

Solving the IBVP given in Eqs. (12) - (14), we get

$$\tau_{yz}=2r, \tag{20}$$

and so

$$\tau=2r_p \tag{21}$$

$$\left.\begin{aligned} u_p=\left[1+2r_p-\frac{8}{3}\sqrt{r_p}-\frac{1}{3}r_p^2\right], 0\leq r\leq r_p\\ u\left(r\right)=\left[\left(1-r^2\right)-\frac{8}{3}\left(1-r^{\frac{3}{2}}\right)\sqrt{r_p}+2r_p\left(1-r\right)\right], \\ r_p\leq r\leq 1 \end{aligned}\right\}, \tag{22}$$

where u_p, is the velocity in the plug flow region, and $u(r)$ is the velocity of the remaining portion of the tube.

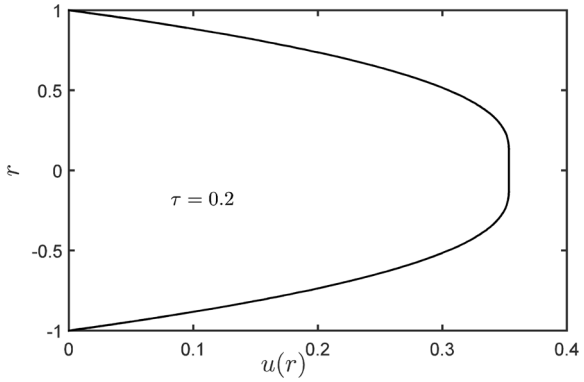

Fig. 2 Velocity Profile

4 Aris-Barton Approach

Following the method of integral moment proposed by Aris [9] and then modified by Barton [10], we define the p-th moment of the distribution of the solute in the filament through r in time t as,

$$C_p\left(t,r\right)=\int_{-\infty}^{+\infty}z^pC\left(t,r,z\right)dz. \tag{23}$$

The average concentration moment over the cross-section of the tube is given by,

$$\bar{C}_p\left(t\right)=\frac{\int_0^{2\pi}d\theta\int_0^1 rC_p\left(t,r\right)dr}{\int_0^{2\pi}d\theta\int_0^1 rdr}. \tag{24}$$

Where overbar denotes the cross-sectional mean.

Using Eq. (23), the diffusion Eq. (15) subject to initial and boundary conditions (17) - (19) can be written as:

$$\begin{aligned}\frac{\partial C_p}{\partial t}-\frac{D^*}{r}\frac{\partial}{\partial r}\left(r\frac{\partial C_p}{\partial r}\right)\\ =-pu\left(r\right)C_{p-1}\\ +\frac{D^*}{Pe^2}p\left(p-1\right)C_{p-2},\end{aligned} \tag{25}$$

with

$$C_p(0,r)=\begin{cases}\dfrac{1}{Pe} & \text{for } p=0\\ 0 & \text{for } p>0\end{cases}\Bigg\}.$$
$$\frac{\partial C_p}{\partial r}=\begin{cases}0 & \text{at } r=0\\ -\beta C_p & \text{at } r=1,\end{cases}\Bigg\} \tag{26}$$

Taking average over the cross-section of the tube, Eqs. (25) and (26) become,

$$\frac{d\bar{C}_p}{dt}=p\overline{u(r)C}_{p-1}+\frac{D^*}{Pe^2}p(p-1)\bar{C}_{p-2} -2D^*\beta C_p(t,1), \tag{27}$$

and

$$\bar{C}_p(0)=\frac{1}{Pe}\ \text{ for } p=0,\ \ \bar{C}_p(0)=0\ \text{ for } p>0. \tag{28}$$

The p-th order central moment of the concentration distribution about the mean can be defined as

$$\mu_p(t)=\frac{\int_0^1\int_0^{2\pi}\int_{-\infty}^{+\infty}r\left(z-z_g\right)^p C(t,r,z)\,dr d\theta dz}{\int_0^1\int_0^{2\pi}\int_{-\infty}^{+\infty}rC(t,r,z)\,dr d\theta dz}, \tag{29}$$

where

$$z_g=\frac{\bar{C}_1}{\bar{C}_0} \tag{30}$$

is the centroid or first moment of the solute and $\bar{C}_0$ represents the total mass of the reactive solute in the whole volume of the tube.

The expressions for central moments can be obtained from Eq. (29) as,

$$\left.\begin{aligned}\mu_2(t)&=\frac{\bar{C}_2}{\bar{C}_0}-z_g^2\\ \mu_3(t)&=\frac{\bar{C}_3}{\bar{C}_0}-3z_g\mu_2-z_g^3\\ \mu_4(t)&=\frac{\bar{C}_4}{\bar{C}_0}-4z_g\mu_3-6z_g^2\mu_2-z_g^4\end{aligned}\right\}. \tag{31}$$

The zeroth central moment is equal to unity and first central moment vanishes. The most important for our study is the second central moment μ_2, which represents the variance of the distribution about the mean position whose rate of change gives the dispersion coefficient.

The exchange coefficient K_0 can be figured from the way that the total mass decays exponentially with time as per the following relation:

$$\bar{C}_0(t)=\bar{C}_0(0)e^{\int_0^t -K_0 dt} \tag{32}$$

As the center of mass moves at a speed equal to the advection speed, the advection coefficient K_1 is given by,

$$-K_1=\frac{dz_g}{dt} \tag{33}$$

Aris [9] showed that the rate of change of variance is proportional to the sum of molecular diffusion coefficient along the axial direction and apparent dispersion coefficient (Taylor dispersion coefficient). Since the axial diffusion is negligible compared to the lateral diffusion, the apparent dispersion coefficient K_2 can be written as

$$K_2=\frac{1}{2}\frac{d\mu_2}{dt}. \tag{34}$$

The coefficient of skewness $v_2\ \left(=\mu_3/\mu_2^{\frac{3}{2}}\right)$ and kurtosis $v_3\ \left(=\mu_4/\mu_2^2-3\right)$ are also important factors for measuring the degree of symmetry and peakedness of the concentration distribution respectively. But in the present study, we have restricted ourselves to the second moment only i.e. μ_2.

As the analytical solution of moment equations (for $p > 1$) subject to the initial and boundary conditions for $\beta \neq 0$ is fairly difficult, a finite difference method based on Crank-Nicholson implicit scheme has been adopted in this paper to solve the set of integral moment equations.

With this motive, we divide the plug region into (M_1-1) equal ingredients, each of length Δr_1 and remaining part of the tube into (M_2-1) equal ingredients, each of length Δr_2 which is represented by the grid point j, so that $j = 1$ corresponds to the $r = 0$, $j = M_2$ corresponds to the boundary of the wall $r = 1$ and $j = M_1$ corresponds to the separation layer of the plug and Casson ($r = r_p$) of the tube, i.e. $r_j = (j-1) \times \Delta r_1$ in plug region and $r_j = r_p + (j-1) \times \Delta r_2$ for other part of the region. The grid factor i identifies time t according to the relationship $t_j = \Delta t \times (i-1)$ so that $i = 1$ corresponds to the time $t = 0$. Δt and Δr are the increments of t and r, respectively. C_p (i,j) indicates the value of C_p on the i-th grid factor along the t -axis and j-th grid point along r-axis. The resulting finite difference equation turns into a process of linear algebraic equation with a tri-diagonal coefficient matrix,

$$P_jC_p(i+1,j+1)+Q_jC_p(i+1,j) +R_jC_p(i+1,j-1)=S_j, \tag{35}$$

Where P_j, Q_j, R_j and S_j are the matrix elements

The finite difference form of the initial condition is:

$$\left.\begin{aligned}C_p(1,j)&=1 \ \text{ for } p=0\\ &=0 \ \text{ for } p>0\end{aligned}\right\}, \tag{36}$$

and that of boundary conditions are

$$\left.\begin{aligned}C_p(i+1,0)&=C_p(i+1,2)\\ C_p(i+1,M_2+1)&=C_p(i+1,M_2-1)\\ &\quad -2\beta\Delta rC_p(i+1,M_2),\end{aligned}\right\}. \tag{37}$$

A MATLAB code has been developed to solve the tri-diagonal coefficient matrix by the method of Thomas algorithm [30]

with the help of prescribed initial and boundary conditions. The steps of computations are:

(i) First, the axial velocity u is computed from Eq. (22).

(ii) The concentration C_p is calculated from Eq. (25) on knowing the values of $u(r)$ at the grid point $(i + 1, j)$.

(iii) Finally the value of $\bar{C}_p$ is calculated from Eq. (24) by applying Simpson's one-third rule, with the known values of $u(r)$ and C_p at the corresponding grid points.

Although the present scheme is linearly stable for any finite values of $\frac{\Delta t}{(\Delta r_1)^2}$ and $\frac{\Delta t}{(\Delta r_2)^2}$, in our analysis, we choose $\Delta t = 0.00001$, $\Delta r_1 = \frac{r_p - 0}{M_1 - 1}$, $\Delta r_2 = \frac{r_p}{M_2 - 1}$ and $Pe = 10^3$.

The behaviour of the concentration distribution might also be acquired from the information of the second, third and four order central moments of the distribution. Utilizing these three moments, it is possible to approximate the mean axial concentration distribution $C_m(z, t)$ of tracers within the flow region with the assistance of Hermite polynomial representation for non-Gaussian curves [12] which is given by,

$$C_m(z,t) = \bar{C}_0(t) e^{-\eta^2} \sum_{n=0}^{\infty} a_n(t) H_n(\eta), \tag{38}$$

where $\eta = \frac{z - z_g}{\sqrt{2\mu_2}}$, $z_g = \frac{\bar{C}_1}{\bar{C}_0}$ and H_i, the Hermite polynomials, satisfy the recurrence relation

$$\left.\begin{aligned} H_{i+1}(\eta) &= 2\eta H_i(\eta) - 2iH_{i-1}(\eta), i = 0,1,2,\ldots \\ H_0(\eta) &= 1. \end{aligned}\right\}. \tag{39}$$

The coefficients a_i's are

$$\left.\begin{aligned} a_0 &= \frac{1}{\sqrt{2\pi\mu_2}}. \\ a_1 &= 0. \\ a_2 &= 0. \\ a_3 &= \frac{\sqrt{2}a_0\nu_2}{24}. \\ a_4 &= \frac{a_0\nu_3}{96}. \end{aligned}\right\}. \tag{40}$$

Therefore, given the statistical parameters in Eq. (31), the concentration distribution can be estimated from Eq. (38) at any given location in the axial direction and time.

5 Sankarasubramanian-Gill Approach

We now follow the Sankarasubramanian and Gill [31] approach to deal with the concentration distribution and assume the following expansion as

$$\begin{aligned} C(r,z,t) = f_0(r,t) C_m(z,t) + f_1(r,t) \frac{\partial C_m}{\partial z} \\ + f_2(r,t) \frac{\partial^2 C_m}{\partial z^2} + \ldots, \end{aligned} \tag{41}$$

where f_k's are to be determined and the dimensionless cross-sectional averaged concentration C_m is given by

$$C_m = C_m(z,t) = \frac{2}{2\pi} \int_0^1 \int_0^{2\pi} C\, r\, dr d\theta. \tag{42}$$

Eq. (41) indicates that the difference in actual and mean concentration can be accounted by the convective and diffusive contributions. Integrating Eq. (15) appropriately (cross-sectional average), we get

$$\frac{\partial C_m}{\partial t} = \sum_{i=0}^{\infty} K_i(t) \frac{\partial^i C_m}{\partial z^i}, \tag{43}$$

where

$$K_0(t) = -2D^* \beta f_0(1,t), \quad \text{(Absorbtion Coefficient)} \tag{44}$$

$$K_1(t) = -2D^* \beta f_1(1,t) - 2\int_0^1 u(r) r f_0(r,t)\, dr, \quad \text{(Convective Coefficient)} \tag{45}$$

$$K_2(t) = \frac{D^*}{Pe^2} - 2D^* \beta f_2(1,t) - 2\int_0^1 u(r) r f_1(r,t)\, dr, \quad \text{(Dispersion Coefficient)} \tag{46}$$

Clearly, the non-zero solute flux at the outer boundary of the wall brings a new term $K_0(t)$. In our analysis we consider only K_0, K_1 and K_2. The contribution of K_3 and the subsequent coefficients are very negligible, Fig. 3 describes the concern.

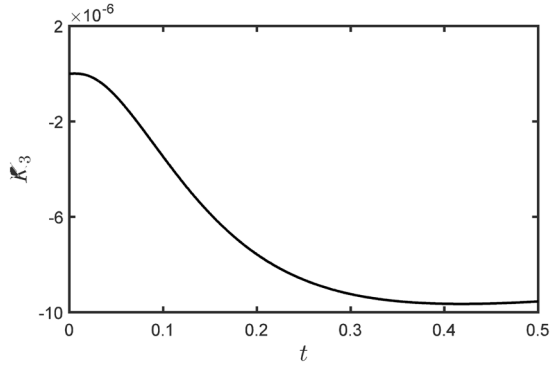

Fig. 3 Plots of K_3 with time

For solving the above coefficients we need to find f_k's. Using the Eq. (41) in Eq. (15) along with Eq. (43) and comparing the coefficients of $\frac{\partial^k C_m}{\partial z^k}$ on either side of the resulting equation, we obtain

$$\begin{aligned} \frac{\partial f_k}{\partial t} + \sum_{i=0}^{k} K_i(t) f_{k-i}(r,t) + u(r) f_{k-1} \\ - \frac{D^*}{r} \frac{\partial}{\partial r}\left(r \frac{\partial f_k}{\partial r} \right) - \frac{D^*}{Pe^2} f_{k-2} = 0, \end{aligned} \tag{47}$$

where $f_{-1} = f_{-2} = 0$ and $k = 0, 1, 2$.

From Eqs. (17) - (19) togather with Eq. (41), the initial conditions for C_m can f_k may be written as:

$$C_m(z,0) = 2\psi(z)\int_0^1 B(r)rdr, \tag{48}$$

$$f_k(r,0) = \begin{Bmatrix} 1 & \text{for} \quad k=0 \\ 0 & \text{for} \; k=1,2 \end{Bmatrix}, \tag{49}$$

$$\frac{\partial f_k}{\partial r} = 0 \;\text{ at }\; r=0 \;\text{ for }\; k=0,1,2, \tag{50}$$

$$\frac{\partial f_k}{\partial r} = -\beta f_k(1,t) \;\text{ at }\; r=1 \;\text{ for }\; k=0,1,2, \tag{51}$$

Also, concentration not reaching far distances downstream, we may write

$$C_m(t,\infty) = \frac{\partial c_m}{\partial z}(t,\infty) = 0. \tag{52}$$

Further, using Eq. (42) in Eq. (41), we get the compatibility condition:

$$\int_0^1 f_k(t,r)rdr = \delta_{k0} \;\text{ for }\; k=0,1,2. \tag{53}$$

To solve the couple Eqs. (44) - (47), we follow the finite difference method based on Crank-Nicholson implicit scheme. The steps of the algorithm are similar to those of the steps discussed in the previous section.

From the Eq. (43) truncating the terms after $K_2(t)$, along with initial and boundary conditions (47)-(52), the solution of C_m is.

$$C_m(t,z) = \frac{1}{2P_e\sqrt{\pi\xi}}\exp\left(\zeta - \frac{z_1^2}{4\xi}\right), \tag{54}$$

Where

$$\zeta(t) = \int_0^t K_0(t)dt, \tag{55}$$

$$z_1(t,z) = z + \int_0^t K_1(t)dt, \tag{56}$$

$$\xi(t) = \int_0^t K_2(t)dt, \tag{57}$$

6 Results and Discussion

The present problem is concerned with longitudinal dispersion of solute subject to molecular diffusion of the solute when introduced into a circular tube. The current model is a very simple version of Casson liquid, however, not beside the point. Fig. 2 shows the common image of liquid velocity profile whilst yield stress τ is 0.2. Relying upon the yield stress, plug region $\mathfrak{R}_p$ is determined, large values of yield stress help to increase the plug core region. In the case of $\tau = 0$, the Casson model will be transformed into Newtonian.

To see the effect of β and τ on the transport coefficients, we follow both Aris-Barton and Sankarasubramanian-Gill approaches. The results outlined in Fig. 4 satisfies a complete qualitative nature of dispersion coefficient obtained from Aris-Barton approach and Sankarasubramanian-Gill approach. This kind of agreement will support the exactness of our computations. Hence, in the rest of our analysis, we confined ourselves to only Aris-Barton's approach.

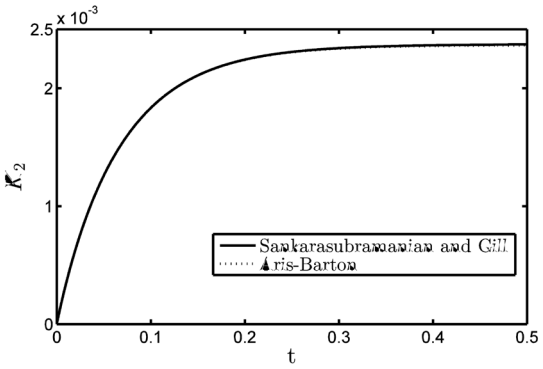

Fig. 4 Comparison between Sankarasubramanian Gill and Aris-Barton approaches

Fig. 5a shows the variation of K_2 with time for different values of β, similarly Fig. 5b represents the same for different yield stresses (τ). The increase in β leads to decrease in the dispersion coefficient, as the increase in β means more solute depleted in the wall and as a result dispersion falls down. An analogous behavior is observed in case of yield stress also. This is due to larger plug region (as yield stress is high) which corresponds lesser velocity gradient near the tube wall ($\mathfrak{R}_c - \mathfrak{R}_p$) and thus dispersion is less.

Variation of asymptotic dispersion coefficient K_2 with respect to β, for different values of yield stress is also examined. As β increases, initially dispersion coefficient increases, but the change is very negligible. Suddenly, there is a decline in dispersion and ultimately reaches in its steady state value. Furthermore, increase in yield stress results in decrease of dispersion coefficient. The reason for such behaviour lies in the fact that the velocity gradient across the solute distribution cause larger axial dispersion, as τ increase means a very less amount of velocity gradient observed near the wall as a result decrease in dispersion coefficient is experienced. Notable that this behavior was observed and explained by Nagarani [24] as well (Fig. 6). Here the steady state is achieved at dimensionless time 0.5.

Fig. 7a shows that there is the variation of negative exchange coefficient $-K_0$ with time for different β. The K_0 gradually increases with the increase of β. When β becomes sufficiently large, the reaction at the wall consumes material more rapidly than it can be supplied by molecular diffusion, as a result diffusion process is stabilized. Fig. 7b shows that the exchange coefficient is independent of the yield stress.

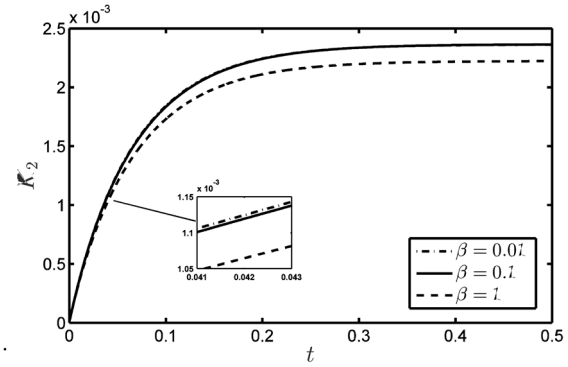

(a) Variation of β with yield stress (τ) = 0.04

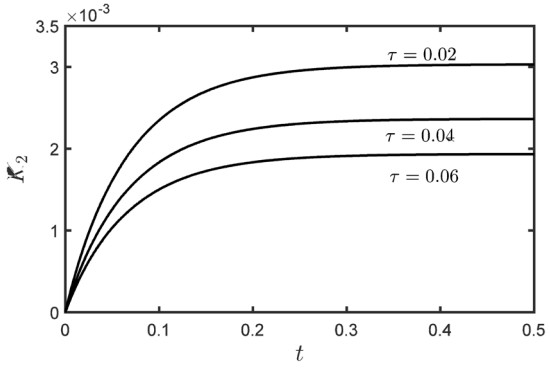

(b) Variation of yield stress (τ) with β = 0.1

Fig. 5 Plots of K_2 with time

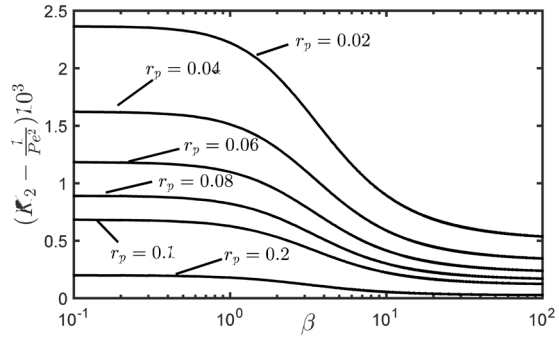

Fig. 6 Variation of β with τ_y = 0.04

Fig. 8a describes the functional relationship between the negative convection coefficient with time with a variety of β. The increase in β rises the negative exchange coefficient. The reason for the enhancement is due to the effect of the wall reaction which deplete solute in the slower moving wall region and, therefore, the solute distribution is weighted in favor of the faster moving central region.

Mean concentration falls with the increase in β (Fig. 9a) and rises with an increase in yield stress (Fig. 9b). The reason of increment or decrement is same as that of K_2.

Although in the above analysis, we have considered an identical diffusivity for the two region viz., in $\mathfrak{R}_p$ and

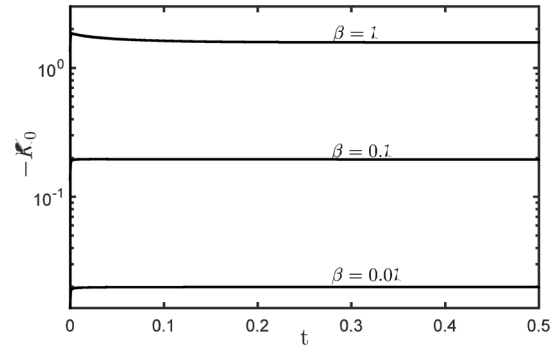

(a) Variation of β with yield stress τ = 0.04

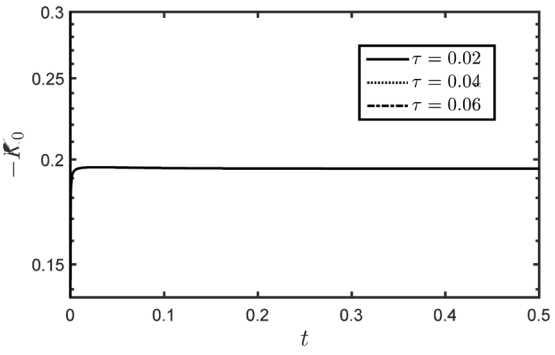

(b) Variation of yield stress (τ) with β = 0.1

Fig. 7 Plots of $-K_0$ with time

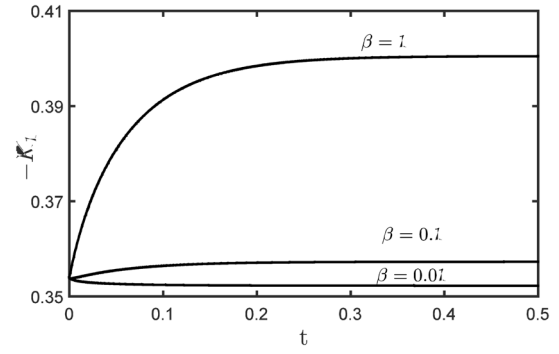

(a) Variation of β with yield stress τ = 0.04

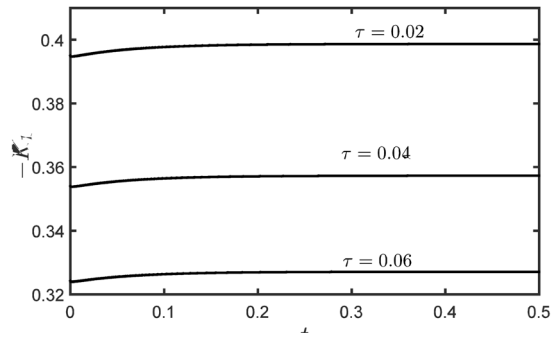

(b) Variation of yield stress (τ) with β = 0.1

Fig. 8 Plots of $-K_1$ with time

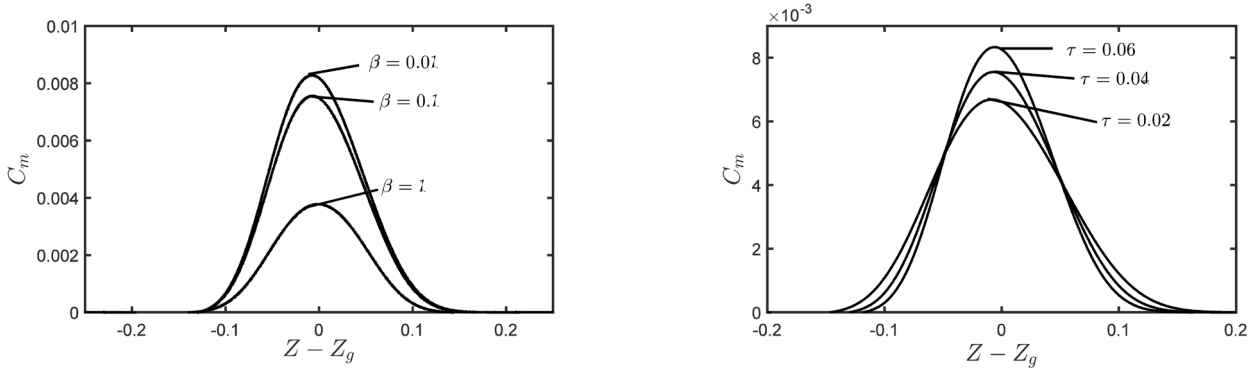

(a) Variation of β with yield stress $\tau = 0.04$

(b) Variation of yield stress (τ) with $\beta = 0.1$

Fig. 9 Plots of Mean Concentration

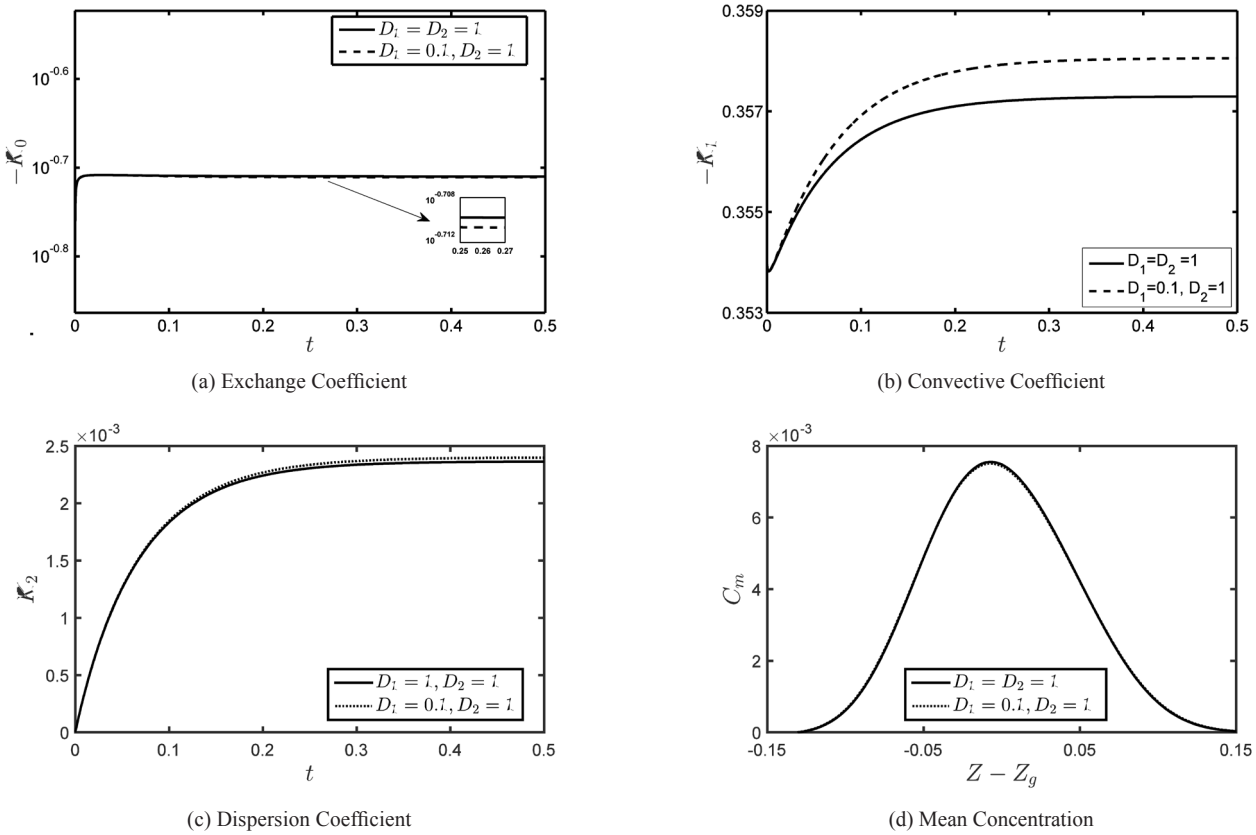

(a) Exchange Coefficient

(b) Convective Coefficient

(c) Dispersion Coefficient

(d) Mean Concentration

Fig. 10 Effects of different diffusivity in different layer on Transport coefficients and Mean concentration with $\tau = 0.04$ and $\beta = 0.1$

$\mathfrak{R}_c - \mathfrak{R}_p$, but our model has the relaxation to choose different diffusivity. In Fig. 10, we see that there's no significant impact of a different diffusing layer on exchange coefficient and mean concentration. It has some impact on convection coefficient and very negligible impact on dispersion coefficient. When the ratio $\frac{D_1}{D_2}$ is high, convection as well as dispersion is less.

7 Conclusion

In this article the longitudinal dispersion of solute is being thoroughly examined. From the evaluation, it is found that the convection coefficient and dispersion coefficient are the functions of wall absorbing parameter β and yield stress τ, however, exchange coefficient simply the function of wall absorbing parameter. Increase of wall absorption, convection and the exchange coefficient increases, but the dispersion coefficient decrease. Yield stress helps to enhance convection coefficient, but reduces dispersion coefficient. Mean concentration also significantly depends on absorption parameter (β) and yield stress (τ). The reliance is as same as that of dispersion coefficient (K_2).

Acknowledgement

I would like to thank MHRD (Ministry of Human Resource Development), India for the financial support to pursue this work. The authors also greatly acknowledge the valuable suggestion by Prof. Pradeep G. Siddheshwar, Bangalore University, Bangalore, India.

References

[1] Harper, R. N., Boyce, C. M., Scott, S. A. "Oxygen carrier dispersion in inert packed beds to improve performance in chemical looping combustion." *Chemical Engineering Journal*. 234, pp. 464–474. 2013. https://doi.org/10.1016/j.cej.2013.08.090

[2] Shaul, S., Kalman, H. "Three plugs model." *Powder Technology*. 283, pp. 579–592. 2015. https://doi.org/10.1016/j.powtec.2015.05.047

[3] Wang, P., Wu, Z., Chen, G., Cui, B. "Environmental dispersion in a three-layer wetland flow with free-surface." *Communications in Nonlinear Science and Numerical Simulation*. 18(12), pp. 3382–3406. 2013. https://doi.org/10.1016/j.cnsns.2013.04.027

[4] Wang, P., Li, Z., Huai, W. X., Chen, B., Li, J. S., Hayat, T., Alsaedi, A., Chen, G. Q. "Indicators for environmental dispersion in a three-layer wetland: Extension of Taylor's classical analysis." *Ecological Indicators*. 47, pp. 254–269. 2014. https://doi.org/10.1016/j.ecolind.2014.04.041

[5] Wu, Z., Chen, G. Q. "Analytical solution for scalar transport in open channel flow: Slow-decaying transient effect." *Journal of Hydrology*. 519, pp. 1974–1984. 2014. https://doi.org/10.1016/j.jhydrol.2014.09.044

[6] Wang, P., Chen, G. Q. "Environmental dispersion in a tidal wetland with sorption by vegetation." *Communications in Nonlinear Science and Numerical Simulation*. 22(1–3), pp. 348–366. 2015. https://doi.org/10.1016/j.cnsns.2014.09.002

[7] Wang, P., Li, Z., Wu, X., An, Y. "Taylor dispersion in a packed pipe with wall reaction: Based on the method of Gill's series solution." *International Journal of Heat and Mass Transfer*. 91, pp. 89–97. 2015. https://doi.org/10.1016/j.ijheatmasstransfer.2015.07.068

[8] Taylor, G. "Dispersion of Soluble Matter in Solvent Flowing Slowly through a Tube." *Proceedings of the Royal Society A: Mathematical, Physical and Engineering Sciences*. 219(1137), pp. 186–203. 1953. https://doi.org/10.1098/rspa.1953.0139

[9] Aris, R. "On the Dispersion of a Solute in a Fluid Flowing through a Tube." *Proceedings of the Royal Society A: Mathematical, Physical and Engineering Sciences*. 235(1200), pp. 67–77. 1956. https://doi.org/10.1098/rspa.1956.0065

[10] Barton, N. G. "On the method of moments for solute dispersion." *Journal of Fluid Mechanics*. 126(1), pp. 205-218. 1983. https://doi.org/10.1017/S0022112083000117

[11] Gill, W. N., Sankarasubramanian, R. "Dispersion of a Non-Uniform Slug in Time-Dependent Flow." *Proceedings of the Royal Society A: Mathematical, Physical and Engineering Sciences*. 322(1548), pp. 101–117. 1971. https://doi.org/10.1098/rspa.1971.0057

[12] Chatwin, P. C. "The approach to normality of the concentration distribution of a solute in a solvent flowing along a straight pipe." *Journal of Fluid Mechanics*. 43(2), pp. 321-352. 1970. https://doi.org/10.1017/S0022112070002409

[13] Purtell, L. P. "Molecular diffusion in oscillating laminar flow in a pipe." *Physics of Fluids*. 24(5), pp. 789-79. 1981. https://doi.org/10.1063/1.863450

[14] Ng, C. O. "Dispersion in steady and oscillatory flows through a tube with reversible and irreversible wall reactions." *Proceedings of the Royal Society A: Mathematical, Physical and Engineering Sciences*. 462(2066), pp. 481–515. 2006. https://doi.org/10.1098/rspa.2005.1582

[15] Mazumder, B. S., Paul, S. "Dispersion of reactive species with reversible and irreversible wall reactions." *Heat and Mass Transfer*. 48(6), pp. 933–944. 2012. https://doi.org/10.1007/s00231-011-0920-7

[16] Paul, S. "Effect of wall oscillation on dispersion in axi-symmetric flows between two coaxial cylinders." *ZAMM - Journal of Applied Mathematics and Mechanics / Zeitschrift für Angewandte Mathematik und Mechanik*. 91(1), pp. 23–37. 2011. https://doi.org/10.1002/zamm.200700106

[17] Pažanin, I. "Modeling of solute dispersion in a circular pipe filled with micropolar fluid." *Mathematical and Computer Modelling*. 57(9–10), pp. 2366–2373. 2013. https://doi.org/10.1016/j.mcm.2011.12.031

[18] Marušić-Paloka, E., Pažanin, I. "On reactive solute transport through a curved pipe." *Applied Mathematics Letters*. 24(6), pp. 878–882. 2011. https://doi.org/10.1016/j.aml.2010.12.039

[19] Charm, S., Kurland, G. "Viscometry of Human Blood for Shear Rates of 0-100,000 sec−1." *Nature*. 206(4984), pp. 617–618. 1965. https://doi.org/10.1038/206617a0

[20] Fan, L. T., Hwang, W. S. "Dispersion of Ostwald-de Waele Fluid in Laminar Flow Through a Cylindrical Tube." *Proceedings of the Royal Society A: Mathematical, Physical and Engineering Sciences*. 283(1395), pp. 576–582. 1965. https://doi.org/10.1098/rspa.1965.0046

[21] Shukla, J. B., Parihar, R. S., Rao, B. R. P. "Dispersion in non-Newtonian fluids: Effects of chemical reaction." *Rheologica Acta*. 18(6), pp. 740–748. 1979. https://doi.org/10.1007/BF01533349

[22] Sharp, M. K. "Shear-augmented dispersion in non-Newtonian fluids." *Annals of Biomedical Engineering*. 21(4), pp. 407–415. 1993. https://doi.org/10.1007/BF02368633

[23] Dash, R. K., Jayaraman, G., Mehta, K. N. "Shear Augmented Dispersion of a Solute in a Casson Fluid Flowing in a Conduit." *Annals of Biomedical Engineering*. 28(4), pp. 373–385. 2000. https://doi.org/10.1114/1.287

[24] Nagarani, P., Sarojamma, G., Jayaraman, G. "Effect of Boundary Absorption in Dispersion in Casson Fluid Flow in a Tube." *Annals of Biomedical Engineering*. 32(5), pp. 706–719. 2004. https://doi.org/10.1023/B:ABME.0000030236.75826.8a

[25] Nagarani, P., Sarojamma, G., Jayaraman, G. "Effect of boundary absorption on dispersion in Casson fluid flow in an annulus: application to catheterized artery." *Acta Mechanica*. 202(1–4), pp. 47–63. 2009. https://doi.org/10.1007/s00707-008-0013-y

[26] Nagarani, P., Sebastian, B. T., Kotsireas, I., Melnik, R., West, B. "Effect of Flow Oscillation on Dispersion of a Solute in a Tube." *AIP Conference Proceedings*. 1368, pp. 29–32. 2011. https://doi.org/10.1063/1.3663452

[27] Nagarani, P., Lewis, A. "Peristaltic flow of a Casson fluid in an annulus." *Korea-Australia Rheology Journal*. 24(1), pp. 1–9. 2012. https://doi.org/10.1007/s13367-012-0001-6

[28] Nagarani, P., Sebastian, B. T. "Dispersion of a solute in pulsatile non-Newtonian fluid flow through a tube." *Acta Mechanica*. 224(3), pp. 571–585. 2013. https://doi.org/10.1007/s00707-012-0753-6

[29] Rana, J., Murthy, P. V. S. N. "Unsteady solute dispersion in non-Newtonian fluid flow in a tube with wall absorption." *Proceedings of the Royal Society A: Mathematical, Physical and Engineering Sciences*. *472*(2193), pp. 20160294. 2016. https://doi.org/10.1098/rspa.2016.0294

[30] Anderson, D. A., Tannehill, J. C., Pletcher, R. H. "*Computational fluid mechanics and heat transfer*." Hemisphere Publishing, New York, 1984.

[31] Sankarasubramanian, R., Gill, W. N. "Unsteady Convective Diffusion with Interphase Mass Transfer." *Proceedings of the Royal Society A: Mathematical, Physical and Engineering Sciences*. 333(1592), pp. 115–132. 1973. https://doi.org/10.1098/rspa.1973.0051